Research Square

Preprints are preliminary reports that have not undergone peer review.
They should not be considered conclusive, used to inform clinical practice,
or referenced by the media as validated information.

# Hydrogen–Deuterium Exchange Mass Spectrometry as a Complementary Approach to X-ray Crystallography and Cryo-EM for Elucidating GPCR Structure and Dynamics

**Minh Duc Nguyen**

duc.nguyenminh@phenikaa-uni.edu.vn

Phenikaa University

**Tan Khanh Nguyen**

Dong A University

**Systematic Review**

**Keywords:** GPCR, HDX-MS, cryo-EM, X-ray crystallography, G-protein, conformational dynamics

**Posted Date:** November 23rd, 2026

**DOI:** https://doi.org/10.21203/rs.3.rs-11553101/v1

**License:** This work is licensed under a Creative Commons Attribution 4.0 International License. Read Full License

**Additional Declarations:** No competing interests reported.

## Abstract

G protein-coupled receptor structures determined by X-ray crystallography and cryogenic electron microscopy have established the atomic basis of ligand recognition and transducer coupling. However, these methods generally characterize selected conformational states and provide limited direct information on regional exchange kinetics and solution-phase conformational behavior. Hydrogen–deuterium exchange mass spectrometry (HDX-MS) complements high-resolution structural approaches by identifying receptor and transducer regions whose backbone protection changes in response to ligands, G proteins, arrestins, accessory proteins, ions, and membrane environments. Pulse-labeling HDX-MS further resolves the temporal progression of conformational changes during receptor–G-protein assembly, nucleotide exchange, and complex dissociation. This review summarizes representative applications of HDX-MS in GPCR research, with particular emphasis on its integration with crystallography, conventional and time-resolved cryo-EM. As peptide-level exchange changes are mechanistically nonunique, the strongest interpretations arise from orthogonal structural, kinetic, and functional validation. HDX-MS should therefore be regarded not as a substitute for high-resolution methods, but as an experimental bridge between GPCR structural states and their solution-phase dynamics.


## 1. Introduction

G protein-coupled receptors (GPCRs) constitute the largest and most diverse superfamily of cell-surface membrane receptors in eukaryotes, with approximately 800 members identified in the human genome (Stevens et al. 2013; Weigelt et al. 2008; Zhang et al. 2024). They are integral membrane proteins that play a pivotal role in intercellular communication by transducing a wide range of extracellular stimuli into intracellular signals (Rosenbaum et al. 2009). GPCRs possess a highly conserved structural architecture consisting of seven transmembrane (7TM) α-helices interconnected by three intracellular loops (ICLs) and three extracellular loops (ECLs). The N-terminus is oriented toward the extracellular space, while the C-terminus is located on the cytoplasmic side of the membrane (Granier and Kobilka 2012; Sutkeviciute and Vilardaga 2020). They sense diverse extracellular signals, including photons (light), ions, lipids, neurotransmitters, hormones, and odorants. When an agonist binds to the receptor, it triggers a conformational change which opens a cavity on the intracellular side to accommodate signaling partners (Zhang et al. 2024). By acting as agonists, antagonists, or allosteric modulators, drugs alter GPCR-mediated signaling and consequently regulate downstream cellular responses (Shoichet and Kobilka 2012).

GPCRs are essential for a wide range of physiological processes, including vision, olfaction, emotional regulation, immune responses, and metabolic control. Dysfunction or mutations in GPCRs are linked to numerous human diseases, such as cardiovascular ailments, neurodegenerative disorders, cancer, obesity, and diabetes (Barella et al. 2021; Grammatopoulos 2017; Huang et al. 2017; Wang et al. 2018). Because of their accessibility at the cell surface and their central role in human pathology, GPCRs are the most prominent drug targets in pharmaceutical research (Hauser et al. 2017; Santos et al. 2017). Currently, approximately 34% of all FDA-approved drugs target GPCRs (Lorente et al. 2025; Sriram and Insel 2018). Structural biology continues to revolutionize this field by providing high-resolution maps of receptor states, which enables structure-based drug design for improved selectivity and reduced side effects (Conflitti et al. 2025; Congreve et al. 2020).

The structural determination of G protein-coupled receptors (GPCRs) has undergone a dramatic revolution, transitioning from an era where membrane proteins were considered highly "refractory" targets to one of routine, high-resolution visualization (Table 1) (Hilger et al. 2018; Rosenbaum et al. 2009; Shonberg et al. 2015). The Table

1 listed methods which haven been applied to investigate GPCR conformations. This evolution has been propelled by the sequential and now complementary breakthroughs in X-ray crystallography and cryo-electron microscopy (cryo-EM) (García-Nafría and Tate 2021; Singh et al. 2026). Despite their transformative contributions, X-ray crystallography and cryo-EM generally enrich selected conformational states and may provide limited information on the kinetics, populations, and solution behavior of GPCR ensembles (Hilger et al. 2018). Flexible loops and terminal regions may remain unresolved, while receptor engineering, stabilizing binders, nucleotide depletion, detergents, and membrane mimetics can influence the states observed experimentally (Latorraca et al. 2016). Cryo-EM classification and variability analysis partially address conformational heterogeneity, but the temporal relationships among reconstructed classes usually require independent kinetic evidence (Lyumkis 2019).

HDX-MS complements X-ray crystallography and cryo-EM by reporting regional changes in backbone protection under solution conditions. Rather than providing atomic coordinates, HDX-MS identifies receptor regions whose conformational behavior changes in response to ligand binding, transducer coupling, accessory proteins, ions, or membrane composition (Englander and Kallenbach 1983; Masson et al. 2019). This review critically evaluates how HDX-MS can validate, extend, and kinetically interpret high-resolution GPCR structures, with particular emphasis on ligand-dependent conformational fingerprints, G-protein coupling, time-resolved activation, and integration with high-resolution structural approaches as well as computational and biophysical methods.

## 2. High-resolution Structural Approaches for GPCRs

# 2.1. X-ray crystallography

X-ray crystallography established the atomic framework for understanding GPCR structure and activation (Kogut-Günthel et al. 2025). The first high-resolution GPCR structure, dark-adapted bovine rhodopsin, was determined in 2000 at 2.8 Å resolution (Palczewski et al. 2000). Subsequent determination of non-rhodopsin GPCR structures required substantial advances in receptor expression, stabilization, purification, and crystallization (Fig. 1). In 2007, structures of the human $\beta_2$-adrenergic receptor provided the first atomic views of a diffusible-ligand-activated GPCR (Cherezov et al. 2007; Rasmussen et al. 2007; Rosenbaum et al. 2007). Following that, the $\beta_2$AR–$G_s$ complex reported in 2011 defined the structural basis of receptor-catalyzed G-protein activation (Rasmussen et al. 2011b). These advances contributed to the award of the 2012 Nobel Prize in Chemistry to Kobilka and Lefkowitz who made extensive contributions to the GPCR field.

These early structures depended on substantial methodological innovation. Fusion partners such as T4 lysozyme and BRIL were introduced into flexible receptor regions to improve stability and facilitate crystal packing (Miyagi et al. 2020; Rosenbaum et al. 2007). Thermostabilizing mutations increased receptor stability in detergent while conformationally selective nanobodies enriched defined functional states (Rasmussen et al. 2011a; Serrano-Vega et al. 2008; Warne et al. 2008). Lipidic cubic phase crystallization provided a membrane-like environment favorable for GPCR crystallization, and microfocus synchrotron beamlines enabled diffraction measurements from small and radiation-sensitive crystals (Caffrey and Cherezov 2009; Cherezov 2011). Although these approaches transformed GPCR structural biology, receptor engineering and conformational stabilization may alter the conformational ensemble recovered experimentally

# 2.2. Cryo-EM

Advances in single-particle cryo-EM, particularly direct electron detection, motion correction, and improved image classification, have transformed GPCR structural biology (Fig. 1). In 2017, the Nobel Prize awarded to three

scientists who helped to develop the cryo-EM technique to image biomacromolecules (Cressey and Callaway 2017). The first GPCR–G-protein cryo-EM structures, including activated calcitonin and GLP-1 receptors, demonstrated the suitability of the method for conformationally heterogeneous signaling complexes (Liang et al. 2017; Zhang et al. 2017b). Since 2018, cryo-EM has become a major platform for determining active-state GPCR structures, particularly receptors assembled with heterotrimeric G-proteins, arrestins, or other binding partners (Russell et al. 2025; Shihoya et al. 2024).

Cryo-EM eliminates the requirement for crystallization and can accommodate receptors in detergents, nanodiscs, and other membrane-mimetic environments (Shihoya et al. 2024). Advances in direct electron detectors, motion correction, and unsupervised three-dimensional classification have further significantly improved image quality and enabled distinct conformational states to be resolved from heterogeneous samples, while phase plates can enhance contrast for smaller targets (Danev et al. 2017; Zivanov et al. 2018). Nevertheless, GPCR cryo-EM still requires sufficiently concentrated, homogeneous, and stable samples. Isolated GPCRs, typically approximately 40 kDa, are often too small for reliable particle alignment; consequently, many studies examine larger complexes containing G-proteins, arrestins, antibodies, or other stabilizing partners (García-Nafría and Tate 2021; Shihoya et al. 2024). These strategies facilitate structural determination but may enrich particular conformational states.

## 2.3. Complementary Information Required to Interpret GPCR Dynamics

HDX-MS measures peptide-level changes in backbone amide exchange that reflect the combined influences of hydrogen bonding, solvent accessibility, intrinsic sequence, and conformational fluctuations (Konermann et al. 2011). Because these ensemble-averaged measurements do not provide atomic coordinates or uniquely identify the structural origin of an uptake change, HDX-MS data are most informative when interpreted within an orthogonal structural and functional framework (Nyvall et al. 2026).

X-ray crystallography and cryo-EM provide three-dimensional templates for mapping differential deuterium uptake onto ligand-binding pockets, transducer interfaces, and activation-associated microswitches (García-Nafría and Tate 2021). HDX-MS complements these structures by reporting on flexible loops, terminal regions, and conformationally heterogeneous segments that may be poorly resolved in structural maps (Chung et al. 2011). Nevertheless, reduced uptake does not necessarily indicate direct binding, as protection may also arise from decreased solvent accessibility, stronger hydrogen bonding, or propagated allosteric stabilization (Vinciauskaite and Masson 2023).

Molecular dynamics simulations can propose atomistic explanations for experimental exchange patterns, while ensemble-reweighting approaches use HDX-MS data to refine the populations of simulated conformations (Konermann and Scrosati 2024). Native MS, lipidomics, NMR, hydroxyl-radical footprinting, and distance-based spectroscopic methods provide complementary information on complex stoichiometry, lipid or ion association, site-specific conformational exchange, side-chain accessibility, and structural distributions (Yen et al. 2023). These techniques help distinguish local interactions from broader changes in receptor dynamics, although computationally inferred residue-level mechanisms remain model dependent.

Table 1
Complementary observables, strengths, and limitations of methods used to characterize GPCR structure and dynamics

| Method | Primary observable | Spatial information | Temporal information | Major contribution to GPCR research | Principal limitations |
|---|---|---|---|---|---|
| X-ray crystallography | Electron-density-derived atomic model | Atomic or near-atomic for ordered regions | No direct kinetic ordering | Defines ligand-binding pockets, receptor microswitches, ion sites, and intermolecular contacts. | Requires crystallization; flexible regions may be unresolved; receptor engineering and conformational stabilization may influence the recovered state. |
| Conventional cryo-EM | Coulomb-potential-derived structural classes | Atomic to near-atomic for sufficiently ordered regions | No direct kinetic ordering | Resolves active GPCR complexes with G-proteins, arrestins, peptide ligands, antibodies, and accessory proteins. | Requires sufficient particle size and homogeneity; flexible regions may remain unresolved; reconstructed classes do not establish temporal order. |
| Time-resolved cryo-EM | Structural populations enriched at defined post-mixing times | Near-atomic for sufficiently populated intermediates | Discrete times after reaction initiation | Visualizes time-dependent structural populations during nucleotide binding, G-protein activation, and complex dissociation. | Limited by mixing and vitrification dead time, particle abundance, and classification; classes may represent parallel or reversible states. |
| Conventional HDX-MS | Peptide-level backbone amide exchange | Usually peptide-level, commonly ~ 5–20 residues | Exchange-time dependence of pre-equilibrated states | Identifies ligand-, transducer-, or environment-sensitive regions and compares conformational ensembles in solution. | Does not provide atomic coordinates; uptake changes are mechanistically nonunique; limited by back-exchange and peptide coverage. |
| Pulse-labeling HDX-MS | Regional protection during a fixed $D_2O$ pulse at defined reaction delays | Peptide-level | Reaction-time dependence using a fixed pulse | Resolves rapid and slow regional changes during GPCR–G-protein assembly, nucleotide exchange, and | Requires precise synchronization and dead-time control; each pulse remains an ensemble-averaged measurement. |

| Method | Primary observable | Spatial information | Temporal information | Major contribution to GPCR research | Principal limitations |
|---|---|---|---|---|---|
| | | | | complex dissociation. | |
| Solution NMR | Site-specific chemical environments and exchange processes | Residue- or probe-specific | Broad range, depending on experiment | Defines conformational populations, exchange kinetics, and ligand-dependent equilibria. | Frequently requires isotopic labeling or site-specific probes; membrane-protein size and stability can restrict application. |
| Hydroxyl-radical footprinting MS | Covalent modification of solvent-accessible side chains | Residue- or regional-level | Microseconds to milliseconds in rapid-footprinting designs | Detects rapid formation of receptor–transducer contacts and complements slower backbone HDX responses. | Reactivity varies among amino acids; oxidation and modification heterogeneity can complicate interpretation. |
| Native MS | Intact mass, stoichiometry, and noncovalent association | No direct 3D coordinates | Limited direct kinetic information | Defines GPCR complex composition, ligand/lipid association, conformational states, and selected ion-binding events. | Gas-phase stability may not fully represent the membrane-embedded complex; heterogeneous samples complicate assignment. |
| Molecular dynamics simulation | Atomistic trajectories generated from a structural model | Atomic | Determined by simulation length and sampling | Proposes atomic mechanisms underlying exchange changes and enables ensemble modeling. | Depends on the starting structure, force field, sampling, and exchange-prediction model; agreement with HDX-MS is not unique. |

## 3. Principles and Workflow of HDX-MS

# 3.1. Principles of HDX-MS

HDX-MS is a powerful biophysical technique used to investigate protein conformational dynamics, higher-order structures, and protein-protein interactions in solution (Konermann et al. 2011). The technique measures the mass increase that occurs when a protein is exposed to a deuterated solvent, tracking how and where deuterium replaces hydrogen along the polypeptide chain. The interpretation of HDX-MS data on studying protein conformation and dynamics are summarized in Table 2.

Backbone amide hydrogens are the primary structural probes in HDX-MS as they exchange over measurable timescales and are distributed throughout the protein, except at proline residues (Englander and Kallenbach 1983). Moreover, the exchange depends mainly on hydrogen bonding, solvent accessibility, and conformational flexibility. As a result, amides buried within stable secondary structures exchange slowly, whereas exposed or flexible regions exchange rapidly (Chalmers et al. 2011).

Interestingly, the intrinsic exchange rate is influenced by pH, temperature, and neighboring amino acids. Exchange is slowest near pH 2.0–2.5, which forms the basis of the HDX-MS quench step, but increases rapidly under physiological conditions due to base catalysis. Higher temperatures further accelerate exchange, making strict control of labeling and processing conditions essential (Wales and Engen 2006).

The Linderstrøm-Lang model describes exchange through transient opening and closing of protein structure (Englander et al. 1997). In EX2 kinetics, rapid closing requires repeated opening events before exchange and produces a single isotopic distribution that gradually shifts to higher mass. In EX1 kinetics, exchange occurs during a relatively long-lived opening event, producing two distinct isotopic populations and often indicating cooperative unfolding or major conformational transitions (Engen 2009).

## 3.2. Standard Bottom-Up HDX-MS Workflow

Bottom-up HDX-MS remains the most widely adopted HDX-MS approach because of its practical accessibility, methodological flexibility, and well-established workflows. Consensus protocols and best-practice guidelines have been developed to standardize procedures from sample preparation and deuterium labeling through mass spectrometric analysis and data interpretation (Masson et al. 2019). The standard HDX-MS workflow consists of six major experimental and analytical steps (Fig. 2, panel A)

Step 1: Deuterium Labeling (Forward Exchange)

The native protein is diluted into excess $D_2O$ buffer under near-physiological conditions. Samples are collected at multiple time points, typically from seconds to hours, to monitor rapidly exchanging flexible regions and slowly exchanging protected regions.

Step 2: Quenching

At each time point, exchange is minimized by rapidly lowering the pH to approximately 2.5 and the temperature to near 0°C. The quench buffer may also contain denaturants and reducing agents to unfold the protein and disrupt disulfide bonds, facilitating subsequent digestion.

Step 3: Proteolytic Digestion

The quenched protein is rapidly digested under acidic, low-temperature conditions, most commonly using immobilized pepsin. Additional acid-active proteases may be included to improve peptide coverage and spatial resolution.

Step 4: Liquid Chromatographic Separation (UPLC)

The resulting peptides are desalted on a trap column and separated by rapid reversed-phase liquid chromatography. The chromatographic system is maintained near 0°C, and short gradients are used to minimize deuterium back-exchange.

Step 5: Mass Spectrometry (MS) detection

Eluting peptides are ionized by electrospray ionization and analyzed using a high-resolution mass spectrometer, commonly a Q-TOF or Orbitrap instrument. Deuterium incorporation is detected as a shift in the peptide isotopic envelope toward higher mass.

Step 6: Data Analysis and Interpretation

Peptides are first identified from an undeuterated reference sample using tandem mass spectrometry. Specialized software then calculates deuterium uptake from the centroid mass shift of each peptide over time. In differential HDX-MS, uptake profiles from two states, such as apo and ligand-bound proteins, are statistically compared and mapped onto a three-dimensional structure to identify regions showing protection or deprotection.

# 3.3. Time-resolved or pulsed-labeling HDX-MS

Pulse-labeling HDX-MS monitors conformational changes during an ongoing biological reaction (Fig. 2, panel B). Unlike continuous-labeling experiments, which compare pre-equilibrated states across different $D_2O$ incubation periods, pulse labeling initiates a reaction and introduces a short, fixed $D_2O$ pulse after defined delay intervals. Each measurement therefore reports the exchange behavior of the ensemble populated at a particular stage of the reaction.

The workflow contains two independent timescales. First, the reaction is initiated at $T_0$, for example by mixing an agonist-bound GPCR with a GDP-bound heterotrimeric G-protein or by adding GTPγS to a preformed complex. The reaction then proceeds for a defined delay, $t_{delay}$, before an aliquot is exposed to a fixed $D_2O$ pulse. The pulse duration is held constant within an experiment and is selected according to the expected protection range and temporal resolution; 10- and 100-s pulses are commonly used examples rather than universal settings (Du et al. 2019; Kim et al. 2020).

Exchange is subsequently quenched under acidic, low-temperature conditions, followed by proteolysis, liquid chromatography, mass-spectrometric detection, and peptide-level uptake analysis as in conventional bottom-up HDX-MS. Plotting uptake against $t_{delay}$ identifies regions that respond rapidly or slowly during the reaction. However, the pulse provides an ensemble-averaged measurement integrated over its duration rather than an instantaneous structural snapshot.

Reliable pulse-labeling measurements require precise control of mixing dead time, temperature, complex occupancy, and reaction synchronization. Mechanistic assignments should be supported by orthogonal kinetic or structural evidence because changes in uptake do not independently define a unique intermediate.

Table 2
Interpretation of common HDX-MS observations in GPCR studies

| HDX-MS observation | Possible biophysical explanations | Directly supported conclusion | Not supported by HDX-MS alone | Recommended validation |
|---|---|---|---|---|
| Reduced deuterium uptake | Reduced accessibility; stronger or more persistent hydrogen bonding; decreased flexibility; steric shielding; allosteric stabilization | The peptide becomes more protected under the tested condition. | Direct ligand contact, formation of a specific secondary structure, or adoption of a unique conformation. | Cryo-EM or crystallography, mutagenesis, docking, NMR, binding assays |
| Increased deuterium uptake | Increased accessibility; weakened hydrogen bonding; increased conformational exchange; destabilization; redistribution toward open states | The peptide becomes less protected under the tested condition. | Complete unfolding, activation, cavity opening, or dissociation of a specific interaction. | Spectroscopy, activity assays, stability measurements, structural analysis |
| Protection near a ligand pocket | Direct ligand shielding or stabilization propagated from the binding site | The region is sensitive to ligand binding. | The affected residues directly contact the ligand. | High-resolution structure, photoaffinity labeling, competition assays, mutagenesis |
| Protection at a receptor–transducer interface | Direct intermolecular shielding or coupling-induced stabilization | Complex formation changes regional protection. | All protected residues form direct intermolecular contacts. | Cryo-EM, cross-linking MS, mutagenesis, native MS |
| Exchange change distant from the binding site | Long-range allostery, altered populations, or global stabilization/destabilization | The perturbation propagates beyond the immediate binding region. | A single defined allosteric pathway. | Mutational networks, MD, NMR, functional rescue |
| Bimodal isotopic envelope | EX1-like exchange; slowly interconverting populations; heterogeneous occupancy; incomplete assembly; carryover or coelution | At least two isotopic populations contribute to the signal. | The identity of each population or definite EX1 kinetics. | Population deconvolution, occupancy controls, carryover assessment, spectroscopy |
| Gradual change across reaction delay | Progressive stabilization/destabilization or change in conformational populations | Regional protection evolves during the monitored process. | A unique sequential reaction mechanism. | Global kinetic fitting, nucleotide-exchange assays, fluorescence, time-resolved cryo-EM |
| Rapid change at the first measurable delay | Fast response within or before the experimental time resolution | The region responds early relative to slower components. | The change is the initiating molecular event. | Shorter delays, dead-time characterization, rapid mixing, kinetic assays |

| HDX-MS observation | Possible biophysical explanations | Directly supported conclusion | Not supported by HDX-MS alone | Recommended validation |
|---|---|---|---|---|
| No significant uptake difference | Similar average exchange; insufficient sensitivity; poor coverage; opposing population changes; incomplete occupancy | No statistically detectable peptide-level change under the tested conditions. | Structural identity or absence of functional effects. | Alternative peptides, higher coverage, occupancy assessment, orthogonal methods |

## 3.4. Technical Limitations and Interpretive Constraints

HDX-MS measurements are affected by deuterium back-exchange during quenching, digestion, chromatography, and ionization (Konermann and Scrosati 2024). Because the extent of back-exchange varies among peptides, absolute uptake values should be interpreted cautiously, particularly when comparing peptides with different sequences or chromatographic retention times. Fully deuterated controls can estimate label recovery but may be difficult to prepare for aggregation-prone membrane proteins.

Spatial resolution in bottom-up HDX-MS is generally limited by peptide length and coverage (Konermann and Scrosati 2024). Overlapping peptides can improve regional localization, but most measurements remain peptide-resolved rather than residue-resolved (Smit et al. 2021). Moreover, the first two residues of each peptide provide limited information because of rapid back-exchange. Changes within a peptide therefore cannot usually be assigned to a specific amide without complementary fragmentation or computational analysis (Table 2).

Differential uptake should be evaluated using biological or independently prepared replicates, predefined significance criteria, and statistical approaches that account for variability across time points (Bradshaw et al. 2020). Because overlapping peptides are not statistically independent, the number of peptide-level differences should not be interpreted as the number of independent structural events. Both uptake magnitude and reproducibility should be reported, preferably with confidence intervals or appropriately corrected significance tests.

GPCR analysis introduces additional complications arising from detergents, lipids, glycosylation, limited protein availability, and incomplete complex assembly (Comamala et al. 2020; Guffick and Politis 2025). Membrane mimetics can alter solvent accessibility and intrinsic exchange behavior, while free detergents and lipids may suppress ionization or compromise chromatography (Guffick and Politis 2025). Differential comparisons should therefore use matched membrane composition, labeling conditions, receptor occupancy, and complex stoichiometry.

Finally, changes in uptake are mechanistically nonunique. Protection may arise from direct binding, increased hydrogen bonding, reduced solvent accessibility, or long-range allosteric stabilization, whereas deprotection may reflect increased accessibility, reduced hydrogen bonding, conformational heterogeneity, or destabilization (Konermann et al. 2011). Mechanistic conclusions should therefore be supported by structural, mutational, kinetic, and functional evidence.

# 4. Applications of HDX-MS in GPCR research

HDX-MS has become an increasingly important approach for investigating GPCR conformational dynamics and interactions in solution (Fig. 3) (Yen et al. 2023). By measuring backbone amide exchange, the method identifies receptor regions whose protection changes following ligand binding, transducer coupling, or alteration of the membrane environment (Chalmers et al. 2011; Masson et al. 2019). GPCR activation and downstream signaling outcomes are dictated by the conformational plasticity of the receptor in solution (Latorraca et al. 2016). As exchange reflects the combined effects of hydrogen bonding, solvent accessibility, intrinsic sequence, and conformational fluctuations, HDX-MS is most informative when comparisons are performed under matched conditions and interpreted alongside structural and functional evidence (Krishnamurthy et al. 2025). The Table 3 summarized main finding and limitation of recent representative studies which applied HDX-MS as a core approach to study conformations of GPCR.

# 4.1. Mapping Ligand Binding Sites and Defining Conformational Fingerprints

HDX-MS can characterize ligand binding by detecting changes in backbone protection and conformational dynamics across the receptor. In selected receptor systems, ligand-specific HDX profiles have distinguished compounds with different efficacy classes or transducer preferences (Fig. 3A). These profiles provide receptor-dependent conformational fingerprints rather than universal signatures of agonism, antagonism, or signaling bias. Unlike static binding-site information, these fingerprints reveal how ligand engagement redistributes receptor dynamics from the extracellular binding pocket to intracellular signaling regions.

The earliest application of HDX-MS to a GPCR, the $\beta_2$-AR, mapped the binding pocket of the inverse agonist carazolol, revealing a highly dynamic intracellular loop 3 (ICL3) and moderately flexible extracellular loop 2 (ECL2) (West et al. 2011; Zhang et al. 2010). Partial agonists, such as dobutamine and salbutamol, produced intermediate HDX profiles, protecting extracellular regions without inducing the pronounced ICL1 deprotection observed with full agonists (Yen et al. 2022). In the turkey $\beta_1$-adrenergic receptor (t$\beta_1$AR), full agonists increase deuterium exchange in intracellular loop 1 (ICL1), whereas antagonists stabilize this region (Toporowska et al. 2024). These contrasting responses, together with mutational and pharmacological evidence, implicate L72 as a ligand-sensitive element associated with receptor activation (Toporowska et al. 2024). Similarly, in the atypical chemokine receptor ACKR3/CXCR7, agonists and inverse agonists produce distinct changes in TM6 dynamics and differentially protect the conserved DRY motif, illustrating how HDX-MS can distinguish alternative activation states in receptors with atypical signaling properties (Otun et al. 2024). In class B receptors like the Glucagon Receptor (GCGR), HDX-MS identified the distinct contact sites of a peptidic antagonist (on the extracellular domain, stalk region, and ECL1) and mapped the binding of small-molecule negative allosteric modulators (Josephs et al. 2021; Yang et al. 2015; Zhang et al. 2017a).

HDX-MS can also help localize ligand-binding regions when combined with complementary exchange measurements. In rod opsin/rhodopsin, integration of backbone amide HDX with site-specific histidine HDX indicated that non-retinoid pharmacological chaperones, including quercetin, myricetin, and chromenone derivatives, engage the orthosteric pocket and stabilize receptor regions affected by misfolding (Pashandi et al. 2026). Collectively, these studies demonstrate that HDX-MS can connect local ligand interactions with receptor-wide conformational changes, thereby providing mechanistic insight into ligand efficacy, signaling bias, and pharmacological rescue. Nevertheless, reduced deuterium uptake may reflect either direct steric protection or

indirect conformational stabilization. As a result, binding-site assignments and signaling interpretations should be supported by structural, mutational, and functional evidence.

## 4.2. Resolving the Temporal Sequence of GPCR–G-Protein Activation

Time-resolved or pulse-labeling HDX-MS extends conventional differential HDX-MS by following conformational changes during receptor–transducer assembly and nucleotide exchange (Fig. 3B) (Du et al. 2019). Studies of $\beta_2$AR–$G_s$ indicate that coupling occurs through kinetically distinct stages rather than a single concerted transition. Receptor ICL2 responds within seconds of G-protein engagement, whereas stabilization of the cytoplasmic end of TM5 and adjacent ICL3 proceeds over considerably longer timescales. These observations distinguish rapid initial recognition from slower maturation of the receptor–G-protein interface (Du et al. 2019).

HDX-MS can simultaneously monitor rearrangements within the G-protein. Receptor coupling alters exchange within the Gα nucleotide-binding pocket, including the P-loop and β6–α5 region, consistent with destabilization of the GDP-bound state. At the receptor-facing side, the C-terminal α5 helix becomes progressively protected as the interface matures. Complementary hydroxyl-radical footprinting suggests that early α5 side-chain contacts precede broader backbone stabilization, supporting a model in which transient receptor–G-protein interactions initiate nucleotide exchange before formation of the fully stabilized complex (Du et al. 2019).

Time-resolved HDX-MS also resolves events following GTP binding (Ahn et al. 2023). Following GTP binding, complementary kinetic measurements indicated rapid complex dissociation, while pulse-labeling HDX-MS detected slower reorganization of the Gα α-helical domain. Integrative modeling further suggested that this transition proceeds through long-lived intermediate populations and can be modulated by MAGE D2 (Ahn et al. 2023). Collectively, these measurements support a multistep model in which nucleotide-pocket destabilization, interface maturation, and post-GTP Gα reorganization occur on distinguishable timescales. GTP binding then triggers rapid complex dissociation, followed by slower reorganization of the $G\alpha_s$ α-helical domain. Time-resolved HDX-MS therefore separates nucleotide exchange, interface maturation, and post-dissociation remodeling as kinetically distinct processes.

## 4.3. Characterizing G-Protein Coupling Selectivity and Interface Dynamics

G-protein association, productive nucleotide exchange, and coupling selectivity are related but distinct properties. HDX-MS can identify coordinated changes at the receptor interface and Gα nucleotide-binding machinery that are consistent with productive complex formation (Fig. 3B). However, receptor-catalyzed activation must be established using nucleotide-exchange or downstream signaling assays, whereas subtype selectivity requires direct comparison of multiple G-proteins under matched experimental conditions.

HDX-MS can distinguish the dynamic signatures associated with coupling to different G-protein subfamilies, thereby providing insight into transducer selectivity. For example, studies of the endothelin type B receptor ($ET_B$) revealed productive conformational responses upon coupling to $G_{i1}$ and $G_q$, but not $G_s$. By simultaneously monitoring changes in the receptor and G-protein, HDX-MS can distinguish receptor–G-protein combinations that generate coordinated changes at the receptor interface and nucleotide-binding machinery from combinations that

produce only partial or localized responses. Whether these complexes are productively activated must be established using nucleotide-exchange or downstream signaling assays (Ham et al. 2024).

Comparative HDX-MS can also differentiate primary from secondary G-protein coupling. Studies of $M_2R$ and $\beta_2AR$ complexes with $G_{oA}$ and $G_{i3}$ suggested that coupling efficiency depends on the interaction between the distal C-terminus of Gα and specific hydrophobic residues in receptor ICL2 (Kim et al. 2020). Comparative studies of class B1 GPCRs further indicate that productive G-protein coupling involves coordinated stabilization of the intracellular receptor cavity and the Gα α5 interface. However, most available HDX-MS datasets evaluate one receptor–G-protein combination rather than directly comparing multiple G-protein subtypes. These studies therefore provide mechanistic information on productive coupling but more limited evidence for subtype selectivity. Systematic comparisons using matched receptor constructs, membrane environments, nucleotide states, and G-protein concentrations will be required to establish general determinants of class B1 coupling preference (Josephs et al. 2021; Nettleton et al. 2026; Sýs et al. 2026; Yang et al. 2015). Thus, HDX-MS can connect local GPCR–G-proteins contacts with global conformational changes, helping define the interface mechanics and activation pathways that underlie transducer selectivity.

Table 3
Representative applications of HDX-MS in GPCR research

| GPCR or complex | Experimental comparison | HDX-MS design | Principal HDX observation | Complementary evidence/method | Mechanistic contribution and interpretive limitation |
|---|---|---|---|---|---|
| Turkey $\beta_1$-adrenergic receptor (Toporowska et al. 2024) | Full agonists, partial agonists, and antagonists | Differential bottom-up HDX-MS | Ligands generated modality-dependent profiles; full agonists increased exchange in ICL1, whereas antagonists stabilized this region. | Mutagenesis and pharmacological characterization | Demonstrated receptor-wide conformational fingerprints associated with ligand modality. The relationship remains receptor- and assay-dependent. |
| ACKR3/CXCR7 (Otun et al. 2024) | Small-molecule agonists and inverse agonists | Differential HDX-MS with computational modeling | Ligands differentially altered TM6 and regions associated with the conserved DRY motif. | Enhanced-sampling MD and functional assays | Connected ligand classes with alternative receptor-dynamic responses. Protection near a motif does not define a unique microswitch configuration. |
| $\beta_2$AR–G□ (Du et al. 2019) | Receptor–G-protein assembly and nucleotide-dependent activation | Pulse-labeling HDX-MS with rapid footprinting and fluorescence | Rapid changes occurred near ICL2 and the Gα nucleotide-binding machinery; α5 and receptor-interface stabilization proceeded more slowly. | Nucleotide-exchange assays, fluorescence, footprinting, and structural models | Separated early nucleotide-pocket destabilization from slower interface maturation. Regional kinetics do not define a unique structural pathway. |

| GPCR or complex | Experimental comparison | HDX-MS design | Principal HDX observation | Complementary evidence/method | Mechanistic contribution and interpretive limitation |
|---|---|---|---|---|---|
| $M_2R/\beta_2AR$ with $G_i/$ proteins (Kim et al. 2020) | Primary $M_2R–G_i/$ versus secondary $\beta_2AR–G_i/$ coupling, including GA and $G_i3$ | Continuous and pulse-labeling HDX-MS with mutagenesis | Primary and secondary coupling produced distinct receptor- and Gα-terminal exchange responses; the distal $G\alpha_i/$ C-terminus and receptor ICL2 contributed differently to productive coupling. | Mutagenesis and G-protein activation assays | Identified dynamic determinants distinguishing primary from secondary $G_i/$ coupling. Pulse-labeling resolved coupling-dependent changes, but productive selectivity still requires functional validation. |
| GPBAR1–G (Castel et al. 2025) | Apo receptor versus G-bound complex | Differential HDX-MS integrated with cryo-EM | Coupling altered protection in intracellular receptor segments and the Gα α5 region. | High-resolution cryo-EM | Linked interface-associated and propagated protection changes to an atomic model. Protection outside a direct interface may reflect allostery. |
| GCGR–RAMP2 (Krishna Kumar et al. 2023) | GCGR alone versus GCGR associated with RAMP2 | Differential HDX-MS | RAMP2 altered exchange in the extracellular domain, TM1, and TM6 and produced evidence of conformational heterogeneity. | Cryo-EM, smFRET, phosphorylation, and G-protein assays | Supported negative allosteric regulation of GCGR. Bimodality indicates multiple populations but does not alone establish EX1 kinetics. |
| $M_2R–\beta$ arrestin (Maharana et al. 2024) | Free β-arrestin versus phosphorylated receptor-loop-bound complex | Differential HDX-MS integrated with cryo-EM | Localized protection occurred in phosphate-sensitive regions of the arrestin N-domain. | Cryo-EM and interaction assays | Supported persistence of a noncanonical hanging interface in solution. Protection does not alone prove direct residue contacts. |
| DARC–chemokine | Receptor alone versus | Comparative differential | Chemokines protected | Cryo-EM and binding studies | Helped explain broad |

| GPCR or complex | Experimental comparison | HDX-MS design | Principal HDX observation | Complementary evidence/method | Mechanistic contribution and interpretive limitation |
|---|---|---|---|---|---|
| complexes (Saha et al. 2024) | complexes with different chemokines | HDX-MS | overlapping extracellular regions, with limited deeper-pocket and intracellular effects. | | chemokine recognition and evaluate allosteric transmission. No detectable change does not establish structural invariance. |

## 4.4. Allosteric Regulation by Accessory Proteins, Ions, and Membrane Environments

Receptor activity-modifying proteins (RAMPs) reshape GPCR conformational ensembles before and after ligand binding. In the GCGR, RAMP2 induced bimodal isotopic distributions in TM1- and TM6-containing peptides, consistent with the presence of slowly interconverting receptor populations (Fig. 3C) (Krishna Kumar et al. 2023). Together with reduced $G_s$-activation measurements, the HDX-MS changes are consistent with RAMP2 shifting the GCGR ensemble toward states less competent for productive coupling (Krishna Kumar et al. 2023).

HDX-MS study of the calcitonin receptor (CTR) show that RAMP1, RAMP2, and RAMP3 produce distinct dynamic signatures before ligand binding (Fairweather et al. 2026). RAMP2 reduced deuterium uptake across substantial portions of the CTR extracellular domain, whereas RAMP3 increases extracellular-domain dynamics while protecting ICL2 and its own intracellular C-terminal region. These isoform-specific patterns indicate that RAMPs preconfigure the receptor ensemble and may direct different activation and signaling trajectories in $AMY_1R$, $AMY_2R$, and $AMY_3R$ (Fairweather et al. 2026). In the CGRP receptor, formed by CTR and RAMP1, HDX-MS further shows that agonist binding stabilizes the extracellular receptor–RAMP interface while altering TM6 dynamics associated with opening of the intracellular transducer-binding cavity.

HDX-MS can reveal conformational coupling between transducer interfaces and conserved ion-binding pockets. In ACKR3/CXCR7, β-arrestin-1 binding increases exchange in TM2 near $Asp^{2.50}$, a key component of the canonical $Na^+$-binding site in class A GPCRs. This response supports long-range communication between the intracellular transducer interface, central ion-binding cavity, and extracellular ligand-binding pocket (Otun et al. 2024). However, HDX-MS does not directly establish ion release or coordination geometry, which requires complementary structural or biophysical approaches. Moreover, HDX-MS also enables comparison of GPCR dynamics in detergents, bicelles, and lipid nanodiscs, revealing how membrane composition affects receptor stability and conformational equilibria (Duc et al. 2015; Guffick and Politis 2025). These measurements reveal how membrane-mimetic composition influences receptor stability, solvent accessibility, and the equilibrium between functional states (Fig. 3C).

Collectively, these applications establish HDX-MS as a powerful approach for defining how accessory proteins, ions, and lipids reshape GPCR conformational landscapes. The technique directly reports changes in local protection and conformational dynamics, whereas assignments of specific functional states require complementary structural and pharmacological validation.

# 5. Integrating HDX-MS with High-Resolution Structural Techniques

## 5.1. Integration with Cryo-EM and X-Ray Crystallography

HDX-MS complements cryo-EM and X-ray crystallography by revealing the solution-phase dynamics underlying high-resolution GPCR structures. Although crystallography and cryo-EM provide detailed coordinates of ligand-binding pockets and receptor–transducer interfaces, the structures often represent conformationally selected or experimentally stabilized states (Shihoya et al. 2024). Moreover, flexible loops, terminal regions, and intrinsically disordered segments may be poorly resolved or absent from structural maps. HDX-MS can probe these regions when adequate peptide coverage is available, thereby distinguishing rigid interaction interfaces from flexible or conformationally heterogeneous regions (Guffick and Politis 2025).

### 5.1.1. Validating interface-associated protection

Subsequently, HDX-MS complements cryo-EM and crystallography by distinguishing stable interaction interfaces from flexible or conformationally heterogeneous regions (Nyvall et al. 2026). A high-resolution 2.5 Å cryo-EM structure of full-length GPBAR1 complexed with heterotrimeric $G_s$ was solved alongside differential HDX-MS achieving over 76% sequence coverage (Castel et al. 2025). In this study, cryo-EM defined the atomic architecture of the receptor–transducer interface, while HDX-MS identified coupling-sensitive regions across the receptor and G-protein. Protection in intracellular receptor segments and the $G\alpha_s$ α5 region was broadly consistent with the cryo-EM interface, whereas additional exchange changes outside direct contact sites suggested propagated stabilization. This example illustrates that agreement between HDX-MS and cryo-EM can validate interface-associated responses while also revealing longer-range conformational effects (Castel et al. 2025). PACAP38 reduced exchange in TM1-, TM5-, and TM7-containing peptides, consistent with protection of the extracellular orthosteric cleft observed in cryo-EM structures (Nettleton et al. 2026).

### 5.1.2. Relating exchange to structural heterogeneity

HDX-MS can also be compared with cryo-EM 3D variability analysis (3DVA), which identifies continuous conformational heterogeneity within single-particle datasets. In the Calcitonin Gene-Related Peptide Receptor (CGRPR) and GCGR-RAMP2 systems, regions displaying the highest amide exchange in HDX-MS (e.g., ECL1 and the ECD) exhibit the greatest structural mobility across principal components in 3DVA (Josephs et al. 2021; Krishna Kumar et al. 2023). Such agreement provides complementary evidence that the observed structural variability persists in solution.

### 5.1.3. Testing atypical complex architectures

HDX-MS complements cryo-EM by validating atypical receptor–arrestin interfaces and characterizing their dynamics in solution. In the $M_2R$–β-arrestin complex, cryo-EM revealed a noncanonical “hanging” configuration in which phosphorylated ICL3 engages the β-arrestin N-domain without extensive receptor-core contacts. HDX-MS detected localized protection within the phosphate-binding regions of the β-arrestin N-domain, supporting the persistence of this interface in solution (Maharana et al. 2024). In the D6R–β-arrestin complex, cryo-EM indicated a receptor-induced transition of the β-arrestin C-tail from a β-strand to an α-helical conformation. Corresponding changes in deuterium uptake provided solution-phase evidence of C-tail remodeling. Comparative HDX-MS further revealed distinct responses between β-arrestin-1 and β-arrestin-2, suggesting that isoform-specific conformational dynamics influence receptor recognition and complex assembly (Maharana et al. 2024).

## 5.1.4. Characterizing unresolved or flexible regions

In the Duffy antigen receptor for chemokines (DARC), variable terminal segments and intracellular loops may be obscured by conformational heterogeneity, whereas HDX-MS can assess their backbone protection and dynamics in solution (Saha et al. 2024). HDX-MS also supported the superficial binding mode observed in the CCL7–DARC cryo-EM structure: chemokine binding primarily protected the extracellular receptor surface, corresponding to chemokine recognition site 1 (CRS1), while deeper regions of the transmembrane pocket remained comparatively accessible and dynamic. Comparative HDX-MS can rapidly measure the protection patterns induced by different ligands, such as CCL2, CCL7, and CXCL8, revealing whether these chemokines engage shared extracellular regions or produce distinct changes in receptor dynamics (Saha et al. 2024). On the other hand, HDX-MS data may be mapped onto AlphaFold or other predicted structural models to visualize dynamic changes across the receptor sequence. This strategy is useful for long intracellular loops, receptor termini, and flexible domains in systems such as GLP-1R–$G_s$ and calcitonin/amylin receptor complexes (Fairweather et al. 2026; Sýs et al. 2026). However, predicted models should serve as visualization and hypothesis-generating frameworks rather than substitutes for experimentally determined structures.

# 5.2. Time-Resolved HDX-MS as a Dynamic Complement to Conventional and Time-Resolved Cryo-EM

Pulse-labeling HDX-MS complements both conventional and time-resolved cryo-EM by adding kinetic and region-specific information to structural models of GPCR–G-protein activation. Conventional cryo-EM studies commonly capture stabilized nucleotide-free complexes and therefore define GPCR–G-protein/arrestin interfaces after substantial complex maturation. By contrast, pulse-labeling HDX-MS can monitor changes associated with initial receptor engagement, nucleotide-pocket destabilization, interface consolidation, GTP binding, and G-protein dissociation in solution.

Integration with freeze-trapping cryo-EM is particularly informative because the methods report different dimensions of the same process. Time-resolved cryo-EM resolves structural populations enriched at selected time points (Kobayashi et al. 2026; Vo et al. 2026). On the other hand, HDX-MS measures the temporal evolution of protection and conformational dynamics within defined receptor and G-protein regions (Du et al. 2019; Kim et al. 2020). During the early phase of coupling, HDX-MS detects rapid changes in receptor ICL2 and the Gα nucleotide-binding pocket, while cryo-EM provides structural models of corresponding early intermediates(Du et al. 2019). Slower HDX changes in the Gα α5 helix, receptor ICL3, and adjacent transmembrane regions indicate that interface maturation continues after GDP release (Du et al. 2019).

The two approaches are also complementary for examining GTP-induced G-protein rearrangements. Pulse-labeling HDX-MS distinguishes rapid subunit dissociation from slower closure of the Gα α-helical domain, whereas time-resolved cryo-EM resolves populations with different domain orientations (Ahn et al. 2023; Papasergi-Scott et al. 2024). This integration links regional solution-phase kinetics with structurally defined conformational states and supports a multistep model of G-protein activation. Nevertheless, cryo-EM classes should not automatically be assigned as consecutive intermediates, because structural heterogeneity may represent parallel, reversible, or off-pathway conformations (Kobayashi et al. 2026; Vo et al. 2026). Assigning a chronological mechanism therefore requires agreement among structural populations, HDX kinetics, nucleotide-exchange measurements, and functional assays.

Direct integration requires more than qualitative agreement between separate studies. Differences in receptor constructs, ligands, transducers, membrane mimetics, temperature, nucleotide conditions, and reaction timing can complicate comparison between HDX-MS and cryo-EM datasets. Future studies should apply both methods to matched preparations and define the effective dead times of mixing, labeling, and vitrification. Such designs would allow structural populations observed by cryo-EM to be compared more rigorously with the regional kinetics measured by HDX-MS.

## 5.3. Integration with Molecular Dynamics and Computational Modeling

HDX-MS measurements can also constrain molecular dynamics simulations by identifying regions that become stabilized, remain flexible, or undergo ligand-dependent conformational exchange (Fig. 3D). Computational methods estimate residue-level protection factors from structural parameters such as hydrogen bonding, solvent exposure, and local atomic contacts. The calculated profiles can then be compared with experimental deuterium uptake to evaluate whether a simulated conformational ensemble is consistent with the HDX-MS data.

Tools such as HDXer apply protection-factor calculations and ensemble reweighting to molecular dynamics trajectories (Bradshaw et al. 2020). In ACKR3/CXCR7, enhanced-sampling simulations were combined with HDX-MS to relate ligand-dependent exchange patterns to alternative binding poses and receptor conformations (Otun et al. 2024). This integration helped explain how different ligands modify TM6, the conserved DRY motif, and other receptor regions involved in activation and signaling.

More advanced integrative frameworks combine HDX-MS with fluorescence measurements and enhanced-sampling simulations to characterize multistep activation pathways. For example, pulse-labeling HDX-MS, tryptophan-induced fluorescence quenching, and metadynamics can be integrated within Bayesian or Markov-state models to describe transient intermediates during activation of the $\beta_2$AR–Gs complex (Ahn et al. 2023). Such approaches can provide structural ensembles and transition probabilities for events such as opening and closing of the Gα α-helical domain.

Nevertheless, residue-level protection factors and conformational ensembles obtained from these analyses are computational interpretations constrained by HDX-MS, not direct residue-level measurements. Their reliability depends on experimental coverage, exchange models, simulation quality, and the assumptions used to relate protein structure to deuterium uptake. Computational conclusions should therefore be evaluated against independent structural, biochemical, and functional evidence.

## 5.4. Integration with Complementary Biophysical Methods

Complementary biophysical methods extend the spatial, temporal, and functional information provided by HDX-MS. Hydroxyl-radical footprinting mass spectrometry measures changes in side-chain solvent accessibility on shorter timescales than conventional HDX-MS (Du et al. 2019). Combining the two methods can therefore separate rapid contact formation from slower changes in backbone hydrogen bonding and structural stabilization. In studies of $\beta_2$AR–Gs coupling, this approach indicated that initial contacts involving the C-terminal α5 helix of $G\alpha_s$ precede broader stabilization of the receptor–G-protein interface (Du et al. 2019).

Mass photometry can be used before HDX-MS or cryo-EM to assess receptor-complex assembly, sample homogeneity, and stoichiometry in membrane-mimetic environments (Castel et al. 2025). This is particularly

valuable for GPCR complexes containing G-proteins, arrestins, RAMPs, antibodies, or stabilizing proteins, where incomplete assembly could complicate the interpretation of exchange patterns. Other mass-spectrometry methods, including native MS, can further define ligand, lipid, or ion binding and determine complex stoichiometry that cannot be established by HDX-MS alone (Yen et al. 2018; Yen et al. 2022).

Finally, cell-based biosensors and functional assays are required to establish the physiological significance of HDX-sensitive regions (Fig. 3D). Techniques such as NanoBiT complementation, second-messenger assays, arrestin-recruitment measurements, and site-directed mutagenesis can test whether receptor regions identified by HDX-MS influence transducer recruitment or signaling efficiency in living cells (Ham et al. 2024). These assays are especially important because altered deuterium uptake may reflect direct interactions, shifts in solvent accessibility, changes in hydrogen bonding, or propagated allosteric effects.

Together, these integrated approaches connect high-resolution structures with solution dynamics, computationally sampled ensembles, complex assembly, and cellular function. HDX-MS serves as an experimental bridge among these methods by identifying dynamic regions, comparing functional states, and constraining mechanistic models (Nyvall et al. 2026). However, changes in deuterium uptake do not independently define atomic contacts or a specific receptor conformation. Mechanistic interpretations are therefore strongest when HDX-MS results are cross-validated using high-resolution structures, molecular simulations, mutagenesis, and functional measurements (James et al. 2022).

## 6. Future Perspectives of HDX-MS in GPCR Structural Dynamics and drug discovery

# 6.1. Dynamics-Guided Drug Discovery

HDX-MS may complement affinity-based screening by determining whether candidate ligands induce distinct receptor-wide conformational responses (Krishnamurthy et al. 2025). Ligand-specific exchange patterns can help differentiate agonists, partial agonists, antagonists, inverse agonists, and potentially biased ligands, while also identifying regions affected by orthosteric or allosteric modulation (Toporowska et al. 2024). Incorporating such conformational fingerprints into secondary screening could prioritize compounds that produce desired functional states rather than relying solely on binding affinity.

However, HDX-MS is not yet a routine high-throughput screening method. Sample consumption, experimental duration, peptide-level resolution, and data-processing requirements generally restrict its use to hit validation, compound comparison, and mechanistic characterization. Moreover, conformational fingerprints cannot independently establish pharmacological efficacy or signaling bias and must be interpreted alongside matched functional assays (Masson et al. 2017).

# 6.2. Integration with Artificial Intelligence and Computational Modeling

The principal future challenge is not simply to combine HDX-MS with additional computational tools, but to establish reproducible methods for evaluating model uncertainty and non-uniqueness. Multiple structural ensembles may reproduce the same peptide-level uptake data, and predicted interfaces may induce indirect protection without representing direct contacts. Benchmark datasets with known conformational transitions,

standardized forward models, and prospective experimental validation will therefore be necessary before HDX-constrained AI or molecular-dynamics workflows can be used routinely in GPCR drug discovery.

HDX-MS can provide experimental constraints for evaluating structures and interfaces predicted by AlphaFold, RoseTTAFold, and related platforms (Nyvall et al. 2026). Changes in protection following complex formation may help assess predicted GPCR interactions with transducers, antibodies, nanobodies, or regulatory proteins (Engen et al. 2021). Nevertheless, HDX-MS does not directly identify atomic contacts, as altered exchange may reflect indirect stabilization, changes in solvent accessibility, or long-range allostery.

Molecular-dynamics simulations and ensemble-reweighting methods can relate peptide-level uptake profiles to possible residue-level conformational changes. HDX-MS may also guide flexible docking and refinement of ligand-binding poses when high-resolution structures are unavailable (Devaurs et al. 2022). These interpretations remain model dependent, however, and are sensitive to structural templates, force fields, sampling, and the assumptions used to calculate protection factors. Therefore, agreement with HDX-MS data supports, but does not solely validate, a predicted structural ensemble.

## 6.3. GPCR Analysis in Native-Like Membranes and Cellular Contexts

Lipid nanodiscs, bicelles, styrene–maleic acid lipid particles, and native membrane vesicles can preserve receptor–lipid interactions that may be disrupted by detergent solubilization (Yen et al. 2023). HDX-MS comparisons across these environments can identify membrane-dependent changes in receptor protection and conformational equilibria, including effects associated with regulatory lipids such as phosphatidylinositol 4,5-bisphosphate (Guffick and Politis 2025; Yen et al. 2022). Nevertheless, lipids and polymers can interfere with digestion, chromatographic separation, and ionization, requiring careful controls and optimized cleanup procedures (Lioupi et al. 2026).

In situ and cellular HDX-MS remain technically challenging because of rapid exchange, complex sample composition, limited receptor abundance, and the need for immediate quenching and processing (Lin et al. 2022; Lioupi et al. 2026). Although proof-of-concept studies support the feasibility of measuring protein dynamics in complex biological environments, routine analysis of endogenous GPCRs in living cells has not yet been established. Progress will require greater sensitivity, selective receptor enrichment, faster processing, and robust methods for distinguishing receptor-derived peptides from the cellular background.

Integration with native MS, cross-linking MS, lipidomics, and functional assays may provide complementary information on complex stoichiometry, interaction networks, lipid binding, post-translational modifications, and signaling activity (Tang and Robinson 2024). No single method captures all these properties simultaneously, however, HDX-MS is therefore most informative as part of an integrative workflow in which changes in receptor dynamics are evaluated against independent structural, biochemical, and pharmacological evidence.

Overall, HDX-MS is likely to assume a broader role in GPCR research, particularly in compound characterization, conformational-state comparison, and validation of structural models. Its utility in routine drug-discovery pipelines will nevertheless depend on overcoming persistent limitations in throughput, spatial resolution, membrane-protein handling, and data interpretation. Future progress is more likely to arise from integration with orthogonal methods than from HDX-MS functioning as a stand-alone structural or screening platform.

## 7. Conclusion

HDX-MS provides information that is complementary to, rather than substitutive for, X-ray crystallography and cryo-EM. High-resolution structures define the architecture of GPCR states and complexes, whereas HDX-MS identifies regions whose protection and conformational behavior change in response to ligands, transducers, accessory proteins, ions, and membrane environments. Time-resolved HDX-MS extends this contribution by separating rapid nucleotide-pocket rearrangements from slower receptor–G-protein interface maturation and post-nucleotide Gα reorganization.

The principal limitation of HDX-MS is that peptide-level exchange changes are mechanistically nonunique and do not independently define atomic contacts or a single conformational state. Conversely, structural classes obtained by crystallography or cryo-EM do not by themselves establish their populations or temporal sequence in solution. The strongest mechanistic models therefore emerge from integration of HDX-MS with high-resolution structures, kinetic measurements, molecular simulations, mutagenesis, and functional pharmacology.

Future progress will depend on improved membrane-protein handling, lower sample requirements, more reliable spatial localization, standardized time-resolved workflows, and rigorous uncertainty analysis. Within these constraints, HDX-MS is well positioned to serve as an experimental bridge between GPCR structural states and their functional dynamics.

## Declarations

# Competing interests

The authors declare no competing interests.

# Author Contribution

Minh Duc Nguyen initiated the topic, drafted the first version of the manuscript. Minh Duc Nguyen and Tan Khanh Nguyen finallized the main manuscript and prepared the figures.

# Acknowledgement

This manuscript is dedicated to the establishment and development of the Vietnamese Biophysical Society.

# Data availability

No datasets were generated or analysed during the current study.

## References

1. Ahn D, Provasi D, Duc NM, Xu J, Salas-Estrada L, Spasic A, Yun MW, Kang J, Gim D, Lee J, Du Y, Filizola M, Chung KY (2023) Gαs slow conformational transition upon GTP binding and a novel Gαs regulator. iScience

26:106603. https://doi.org/https://doi.org/10.1016/j.isci.2023.106603

2. Barella LF, Jain S, Kimura T, Pydi SP (2021) Metabolic roles of G protein-coupled receptor signaling in obesity and type 2 diabetes. The FEBS Journal 288:2622–2644. https://doi.org/https://doi.org/10.1111/febs.15800
3. Bradshaw RT, Marinelli F, Faraldo-Gómez JD, Forrest LR (2020) Interpretation of HDX Data by Maximum-Entropy Reweighting of Simulated Structural Ensembles. Biophys J 118:1649–1664. https://doi.org/10.1016/j.bpj.2020.02.005
4. Caffrey M, Cherezov V (2009) Crystallizing membrane proteins using lipidic mesophases. Nat Protoc 4:706–731. https://doi.org/10.1038/nprot.2009.31
5. Castel J, Botzanowski T, Brooks I, Frechard A, Bey G, Schroeter M, Del Nero E, Debaene F, Ciesielski F, Zeyer D, Cianferani S, Morales R (2025) Deciphering molecular determinants of GPBAR1-Gs protein interactions by HDX-MS and cryo-EM. Sci Rep 15:31517. https://doi.org/10.1038/s41598-025-16529-w
6. Chalmers MJ, Busby SA, Pascal BD, West GM, Griffin PR (2011) Differential hydrogen/deuterium exchange mass spectrometry analysis of protein–ligand interactions. Expert Review of Proteomics 8:43–59. https://doi.org/10.1586/epr.10.109
7. Cherezov V (2011) Lipidic cubic phase technologies for membrane protein structural studies. Curr Opin Struct Biol 21:559–566. https://doi.org/https://doi.org/10.1016/j.sbi.2011.06.007
8. Cherezov V, Rosenbaum DM, Hanson MA, Rasmussen SGF, Thian FS, Kobilka TS, Choi H-J, Kuhn P, Weis WI, Kobilka BK, Stevens RC (2007) High-Resolution Crystal Structure of an Engineered Human β2-Adrenergic G Protein–Coupled Receptor. Science 318:1258–1265. https://doi.org/10.1126/science.1150577
9. Chung KY, Rasmussen SGF, Liu T, Li S, DeVree BT, Chae PS, Calinski D, Kobilka BK, Woods VL, Sunahara RK (2011) Conformational changes in the G protein Gs induced by the β2 adrenergic receptor. Nature 477:611–615. https://doi.org/10.1038/nature10488
10. Comamala G, Madsen JB, Voglmeir J, Du Y-M, Jensen PF, Østerlund EC, Trelle MB, Jørgensen TJD, Rand KD (2020) Deglycosylation by the Acidic Glycosidase PNGase H+ Enables Analysis of N–Linked Glycoproteins by Hydrogen/Deuterium Exchange Mass Spectrometry. Journal of the American Society for Mass Spectrometry 31:2305–2312. https://doi.org/10.1021/jasms.0c00258
11. Conflitti P, Lyman E, Sansom MSP, Hildebrand PW, Gutiérrez-de-Terán H, Carloni P, Ansell TB, Yuan S, Barth P, Robinson AS, Tate CG, Gloriam D, Grzesiek S, Eddy MT, Prosser S, Limongelli V (2025) Functional dynamics of G protein-coupled receptors reveal new routes for drug discovery. Nature Reviews Drug Discovery 24:251–275. https://doi.org/10.1038/s41573-024-01083-3
12. Congreve M, de Graaf C, Swain NA, Tate CG (2020) Impact of GPCR Structures on Drug Discovery. Cell 181:81–91. https://doi.org/10.1016/j.cell.2020.03.003
13. Cressey D, Callaway E (2017) Cryo-electron microscopy wins chemistry Nobel. Nature 550:167–167. https://doi.org/10.1038/nature.2017.22738
14. Danev R, Tegunov D, Baumeister W (2017) Using the Volta phase plate with defocus for cryo-EM single particle analysis. eLife 6:e23006. https://doi.org/10.7554/eLife.23006
15. Devaurs D, Antunes DA, Borysik AJ (2022) Computational Modeling of Molecular Structures Guided by Hydrogen-Exchange Data. Journal of the American Society for Mass Spectrometry 33:215–237. https://doi.org/10.1021/jasms.1c00328
16. Du Y, Duc NM, Rasmussen SGF, Hilger D, Kubiak X, Wang L, Bohon J, Kim HR, Wegrecki M, Asuru A, Jeong KM, Lee J, Chance MR, Lodowski DT, Kobilka BK, Chung KY (2019) Assembly of a GPCR-G Protein Complex. Cell

177:1232–1242.e1211. https://doi.org/https://doi.org/10.1016/j.cell.2019.04.022

17. Duan J, Liu H, Zhao F, Yuan Q, Ji Y, Cai X, He X, Li X, Li J, Wu K, Gao T, Zhu S, Lin S, Wang M-W, Cheng X, Yin W, Jiang Y, Yang D, Xu HE (2023) GPCR activation and GRK2 assembly by a biased intracellular agonist. Nature 620:676–681. https://doi.org/10.1038/s41586-023-06395-9
18. Duc NM, Du Y, Thorsen TS, Lee SY, Zhang C, Kato H, Kobilka BK, Chung KY (2015) Effective Application of Bicelles for Conformational Analysis of G Protein-Coupled Receptors by Hydrogen/Deuterium Exchange Mass Spectrometry. Journal of the American Society for Mass Spectrometry 26:808–817. https://doi.org/10.1007/s13361-015-1083-4
19. Engen JR (2009) Analysis of Protein Conformation and Dynamics by Hydrogen/Deuterium Exchange MS. Anal Chem 81:7870–7875. https://doi.org/10.1021/ac901154s
20. Engen JR, Botzanowski T, Peterle D, Georgescauld F, Wales TE (2021) Developments in Hydrogen/Deuterium Exchange Mass Spectrometry. Anal Chem 93:567–582. https://doi.org/10.1021/acs.analchem.0c04281
21. Englander SW, Kallenbach NR (1983) Hydrogen exchange and structural dynamics of proteins and nucleic acids. Q Rev Biophys 16:521–655. https://doi.org/10.1017/S0033583500005217
22. Englander SW, Mayne L, Bai Y, Sosnick TR (1997) Hydrogen exchange: The modern legacy of Linderstrøm-Lang. Protein Sci 6:1101–1109. https://doi.org/https://doi.org/10.1002/pro.5560060517
23. Fairweather CJ, Zhang X, Fernando CD, Garama DJ, Sexton PM, Wootten D, Josephs TM (2026) Conformational Dynamics of Amylin Receptors Revealed by Hydrogen–Deuterium Exchange Mass Spectrometry. Journal of the American Chemical Society 148:16702–16712. https://doi.org/10.1021/jacs.5c20644
24. García-Nafría J, Tate CG (2021) Structure determination of GPCRs: cryo-EM compared with X-ray crystallography. Biochem Soc Trans 49:2345–2355. https://doi.org/10.1042/BST20210431
25. Grammatopoulos DK (2017) Regulation of G-protein coupled receptor signalling underpinning neurobiology of mood disorders and depression. Molecular and Cellular Endocrinology 449:82–89. https://doi.org/https://doi.org/10.1016/j.mce.2017.02.013
26. Granier S, Kobilka B (2012) A new era of GPCR structural and chemical biology. Nat Chem Biol 8:670–673. https://doi.org/10.1038/nchembio.1025
27. Guffick C, Politis A (2025) HDX-MS in micelles and membranes for small molecule and biopharmaceutical development. Curr Opin Struct Biol 94:103077. https://doi.org/https://doi.org/10.1016/j.sbi.2025.103077
28. Ham D, Shihoya W, Nureki O, Inoue A, Chung KY (2024) Molecular mechanism of the endothelin receptor type B interactions with Gs, Gi, and Gq. Structure 32:1632–1639.e1634. https://doi.org/10.1016/j.str.2024.06.020
29. Hauser AS, Attwood MM, Rask-Andersen M, Schiöth HB, Gloriam DE (2017) Trends in GPCR drug discovery: new agents, targets and indications. Nature Reviews Drug Discovery 16:829–842. https://doi.org/10.1038/nrd.2017.178
30. Hilger D, Masureel M, Kobilka BK (2018) Structure and dynamics of GPCR signaling complexes. Nat Struct Mol Biol 25:4–12. https://doi.org/10.1038/s41594-017-0011-7
31. Huang Y, Todd N, Thathiah A (2017) The role of GPCRs in neurodegenerative diseases: avenues for therapeutic intervention. Current Opinion in Pharmacology 32:96–110. https://doi.org/https://doi.org/10.1016/j.coph.2017.02.001
32. James EI, Murphree TA, Vorauer C, Engen JR, Guttman M (2022) Advances in Hydrogen/Deuterium Exchange Mass Spectrometry and the Pursuit of Challenging Biological Systems. Chem Rev 122:7562–7623.

https://doi.org/10.1021/acs.chemrev.1c00279

33. Josephs TM, Belousoff MJ, Liang Y-L, Piper SJ, Cao J, Garama DJ, Leach K, Gregory KJ, Christopoulos A, Hay DL, Danev R, Wootten D, Sexton PM (2021) Structure and dynamics of the CGRP receptor in apo and peptide-bound forms. Science 372:eabf7258. https://doi.org/10.1126/science.abf7258
34. Kim HR, Xu J, Maeda S, Duc NM, Ahn D, Du Y, Chung KY (2020) Structural mechanism underlying primary and secondary coupling between GPCRs and the Gi/o family. Nat Commun 11:3160. https://doi.org/10.1038/s41467-020-16975-2
35. Kobayashi K, Kawakami K, Matsui TE, Yokoi S, Fukuda M, Narita TJ, Arai H, Tambo M, Sumikama T, Tatsumi M, Yamashita K, Koyanagi J, Kugawa M, Ikeda H, Sumino A, Mitsutake A, Kobilka BK, Inoue A, Kato HE (2026) The dynamic basis of G-protein recognition and activation by a GPCR. Nature 652:812–821. https://doi.org/10.1038/s41586-026-10228-w
36. Kogut-Günthel MM, Zara Z, Nicoli A, Steuer A, Lopez-Balastegui M, Selent J, Karanth S, Koehler M, Ciancetta A, Abiko LA, Hagn F, Di Pizio A (2025) The path to the G protein-coupled receptor structural landscape: Major milestones and future directions. Br J Pharmacol 182:3225–3248. https://doi.org/https://doi.org/10.1111/bph.17314
37. Konermann L, Pan J, Liu Y-H (2011) Hydrogen exchange mass spectrometry for studying protein structure and dynamics. Chem Soc Rev 40:1224–1234. https://doi.org/10.1039/c0cs00113a
38. Konermann L, Scrosati PM (2024) Hydrogen/Deuterium Exchange Mass Spectrometry: Fundamentals, Limitations, and Opportunities. Mol Cell Proteomics 23:100853. https://doi.org/https://doi.org/10.1016/j.mcpro.2024.100853
39. Krishna Kumar K, O'Brien ES, Habrian CH, Latorraca NR, Wang H, Tuneew I, Montabana E, Marqusee S, Hilger D, Isacoff EY, Mathiesen JM, Kobilka BK (2023) Negative allosteric modulation of the glucagon receptor by RAMP2. Cell 186:1465–1477.e1418. https://doi.org/10.1016/j.cell.2023.02.028
40. Krishnamurthy S, Musgaard M, Tehan BG, Jazayeri A, Liko I (2025) The evolving role of hydrogen/deuterium exchange mass spectrometry in early-stage drug discovery. Curr Opin Struct Biol 92:103051. https://doi.org/https://doi.org/10.1016/j.sbi.2025.103051
41. Latorraca NR, Venkatakrishnan AJ, Dror RO (2016) GPCR Dynamics: Structures in Motion. Chem Rev 117:139–155. https://doi.org/10.1021/acs.chemrev.6b00177
42. Liang Y-L, Khoshouei M, Radjainia M, Zhang Y, Glukhova A, Tarrasch J, Thal DM, Furness SGB, Christopoulos G, Coudrat T, Danev R, Baumeister W, Miller LJ, Christopoulos A, Kobilka BK, Wootten D, Skiniotis G, Sexton PM (2017) Phase-plate cryo-EM structure of a class B GPCR–G-protein complex. Nature 546:118–123. https://doi.org/10.1038/nature22327
43. Lin X, Zmyslowski AM, Gagnon IA, Nakamoto RK, Sosnick TR (2022) Development of in vivo HDX-MS with applications to a TonB-dependent transporter and other proteins. Protein Sci 31:e4402. https://doi.org/https://doi.org/10.1002/pro.4402
44. Lioupi A, Gavriilidou AFM, Politis A (2026) Probing protein–lipid interactions by hydrogen/deuterium exchange-mass spectrometry: advances, challenges and future directions. Chemical Science 17:16599–16614. https://doi.org/10.1039/d6sc04457c
45. Lorente JS, Sokolov AV, Ferguson G, Schiöth HB, Hauser AS, Gloriam DE (2025) GPCR drug discovery: new agents, targets and indications. Nature Reviews Drug Discovery 24:458–479. https://doi.org/10.1038/s41573-025-01139-y

46. Lyumkis D (2019) Challenges and opportunities in cryo-EM single-particle analysis. J Biol Chem 294:5181–5197. https://doi.org/https://doi.org/10.1074/jbc.REV118.005602
47. Maharana J, Sano FK, Sarma P, Yadav MK, Duan L, Stepniewski TM, Chaturvedi M, Ranjan A, Singh V, Saha S, Mahajan G, Chami M, Shihoya W, Selent J, Chung KY, Banerjee R, Nureki O, Shukla AK (2024) Molecular insights into atypical modes of β-arrestin interaction with seven transmembrane receptors. Science 383:101–108. https://doi.org/10.1126/science.adj3347
48. Masson GR, Burke JE, Ahn NG, Anand GS, Borchers C, Brier S, Bou-Assaf GM, Engen JR, Englander SW, Faber J, Garlish R, Griffin PR, Gross ML, Guttman M, Hamuro Y, Heck AJR, Houde D, Iacob RE, Jørgensen TJD, Kaltashov IA, Klinman JP, Konermann L, Man P, Mayne L, Pascal BD, Reichmann D, Skehel M, Snijder J, Strutzenberg TS, Underbakke ES, Wagner C, Wales TE, Walters BT, Weis DD, Wilson DJ, Wintrode PL, Zhang Z, Zheng J, Schriemer DC, Rand KD (2019) Recommendations for performing, interpreting and reporting hydrogen deuterium exchange mass spectrometry (HDX-MS) experiments. Nat Methods 16:595–602. https://doi.org/10.1038/s41592-019-0459-y
49. Masson GR, Jenkins ML, Burke JE (2017) An overview of hydrogen deuterium exchange mass spectrometry (HDX-MS) in drug discovery. Expert Opinion on Drug Discovery 12:981–994. https://doi.org/10.1080/17460441.2017.1363734
50. Miyagi H, Asada H, Suzuki M, Takahashi Y, Yasunaga M, Suno C, Iwata S, Saito J-i (2020) The discovery of a new antibody for BRIL-fused GPCR structure determination. Sci Rep 10:11669. https://doi.org/10.1038/s41598-020-68355-x
51. Nettleton TJ, Fairweather C, Piper SJ, Ishii K, Garama DJ, Sexton PM, Josephs TM, Wootten D (2026) Dynamics of the PAC1 receptor in apo, peptide agonist-bound, and G protein complexed states. Structure 34:814–827.e814. https://doi.org/https://doi.org/10.1016/j.str.2026.01.017
52. Nyvall Hunter G, Shaw Alexandria L, Walsh Emma E, Bhatti H, Burke John E (2026) Use of hydrogen deuterium exchange mass spectrometry in tandem with modern structural biology. Biochemical Journal 483:585–602. https://doi.org/10.1042/BCJ20250131
53. Otun O, Aljamous C, Del Nero E, Arimont-Segura M, Bosma R, Zarzycka B, Girbau T, Leyrat C, de Graaf C, Leurs R, Durroux T, Granier S, Cong X, Bechara C (2024) Conformational dynamics underlying atypical chemokine receptor 3 activation. Proc Natl Acad Sci USA 121:e2404000121. https://doi.org/10.1073/pnas.2404000121
54. Palczewski K, Kumasaka T, Hori T, Behnke CA, Motoshima H, Fox BA, Trong IL, Teller DC, Okada T, Stenkamp RE, Yamamoto M, Miyano M (2000) Crystal Structure of Rhodopsin: A G Protein-Coupled Receptor. Science 289:739–745. https://doi.org/10.1126/science.289.5480.739
55. Papasergi-Scott MM, Pérez-Hernández G, Batebi H, Gao Y, Eskici G, Seven AB, Panova O, Hilger D, Casiraghi M, He F, Maul L, Gmeiner P, Kobilka BK, Hildebrand PW, Skiniotis G (2024) Time-resolved cryo-EM of G-protein activation by a GPCR. Nature 629:1182–1191. https://doi.org/10.1038/s41586-024-07153-1
56. Pashandi Z, Ortega JT, Miyagi M, Golczak M, Jastrzebska B (2026) Conformational signatures of native ligand and pharmacochaperone binding in rhodopsin. Structure 34:1390–1404.e1394. https://doi.org/10.1016/j.str.2026.07.010
57. Rasmussen SGF, Choi H-J, Fung JJ, Pardon E, Casarosa P, Chae PS, DeVree BT, Rosenbaum DM, Thian FS, Kobilka TS, Schnapp A, Konetzki I, Sunahara RK, Gellman SH, Pautsch A, Steyaert J, Weis WI, Kobilka BK (2011a) Structure of a nanobody-stabilized active state of the β2 adrenoceptor. Nature 469:175–180. https://doi.org/10.1038/nature09648

58. Rasmussen SGF, Choi H-J, Rosenbaum DM, Kobilka TS, Thian FS, Edwards PC, Burghammer M, Ratnala VRP, Sanishvili R, Fischetti RF, Schertler GFX, Weis WI, Kobilka BK (2007) Crystal structure of the human β2 adrenergic G-protein-coupled receptor. Nature 450:383–387. https://doi.org/10.1038/nature06325
59. Rasmussen SGF, DeVree BT, Zou Y, Kruse AC, Chung KY, Kobilka TS, Thian FS, Chae PS, Pardon E, Calinski D, Mathiesen JM, Shah STA, Lyons JA, Caffrey M, Gellman SH, Steyaert J, Skiniotis G, Weis WI, Sunahara RK, Kobilka BK (2011b) Crystal structure of the β2 adrenergic receptor–Gs protein complex. Nature 477:549–555. https://doi.org/10.1038/nature10361
60. Rosenbaum DM, Cherezov V, Hanson MA, Rasmussen SGF, Thian FS, Kobilka TS, Choi H-J, Yao X-J, Weis WI, Stevens RC, Kobilka BK (2007) GPCR Engineering Yields High-Resolution Structural Insights into β2-Adrenergic Receptor Function. Science 318:1266–1273. https://doi.org/10.1126/science.1150609
61. Rosenbaum DM, Rasmussen SGF, Kobilka BK (2009) The structure and function of G-protein-coupled receptors. Nature 459:356–363. https://doi.org/10.1038/nature08144
62. Russell IC, Lee D, Wootten D, Sexton PM, Bumbak F (2025) Cryoelectron microscopy as a tool for illuminating activation mechanisms of human class A orphan G protein-coupled receptors. Pharmacol Rev 77:100056. https://doi.org/https://doi.org/10.1016/j.pharmr.2025.100056
63. Saha S, Khanppnavar B, Maharana J, Kim H, Carino CMC, Daly C, Houston S, Sharma S, Zaidi N, Dalal A, Mishra S, Ganguly M, Tiwari D, Kumari P, Jhingan GD, Yadav PN, Plouffe B, Inoue A, Chung KY, Banerjee R, Korkhov VM, Shukla AK (2024) Molecular mechanism of distinct chemokine engagement and functional divergence of the human Duffy antigen receptor. Cell 187:4751–4769.e4725. https://doi.org/10.1016/j.cell.2024.07.005
64. Santos R, Ursu O, Gaulton A, Bento AP, Donadi RS, Bologa CG, Karlsson A, Al-Lazikani B, Hersey A, Oprea TI, Overington JP (2017) A comprehensive map of molecular drug targets. Nature Reviews Drug Discovery 16:19–34. https://doi.org/10.1038/nrd.2016.230
65. Serrano-Vega MJ, Magnani F, Shibata Y, Tate CG (2008) Conformational thermostabilization of the β1-adrenergic receptor in a detergent-resistant form. Proc Natl Acad Sci USA 105:877–882. https://doi.org/10.1073/pnas.0711253105
66. Shihoya W, Iwama A, Sano FK, Nureki O (2024) Cryo-EM advances in GPCR structure determination. The Journal of Biochemistry 176:1–10. https://doi.org/10.1093/jb/mvae029
67. Shoichet BK, Kobilka BK (2012) Structure-based drug screening for G-protein-coupled receptors. Trends Pharmacol Sci 33:268–272. https://doi.org/https://doi.org/10.1016/j.tips.2012.03.007
68. Shonberg J, Kling RC, Gmeiner P, Löber S (2015) GPCR crystal structures: Medicinal chemistry in the pocket. Biorg Med Chem 23:3880–3906. https://doi.org/https://doi.org/10.1016/j.bmc.2014.12.034
69. Singh SK, Agrawal M, Pattanayak A, Baidya M, Kumari P (2026) Strategic advances for cryo-EM structural studies of small (< 100 kDa) GPCRs. Commun Biol 9:237. https://doi.org/10.1038/s42003-026-09516-y
70. Smit JH, Krishnamurthy S, Srinivasu BY, Parakra R, Karamanou S, Economou A (2021) Probing Universal Protein Dynamics Using Hydrogen–Deuterium Exchange Mass Spectrometry-Derived Residue-Level Gibbs Free Energy. Anal Chem 93:12840–12847. https://doi.org/10.1021/acs.analchem.1c02155
71. Sriram K, Insel PA (2018) G Protein-Coupled Receptors as Targets for Approved Drugs: How Many Targets and How Many Drugs? Mol Pharmacol 93:251–258. https://doi.org/10.1124/mol.117.111062
72. Staus DP, Hu H, Robertson MJ, Kleinhenz ALW, Wingler LM, Capel WD, Latorraca NR, Lefkowitz RJ, Skiniotis G (2020) Structure of the M2 muscarinic receptor–β-arrestin complex in a lipid nanodisc. Nature 579:297–302.

https://doi.org/10.1038/s41586-020-1954-0

73. Stevens RC, Cherezov V, Katritch V, Abagyan R, Kuhn P, Rosen H, Wüthrich K (2013) The GPCR Network: a large-scale collaboration to determine human GPCR structure and function. Nature Reviews Drug Discovery 12:25–34. https://doi.org/10.1038/nrd3859
74. Sutkeviciute I, Vilardaga J-P (2020) Structural insights into emergent signaling modes of G protein–coupled receptors. J Biol Chem 295:11626–11642. https://doi.org/https://doi.org/10.1074/jbc.REV120.009348
75. Sýs J, Ho JD, Showalter AD, Yu A-P, Wainscott DB, Laos V, Broughton H, Sloop KW, Espada A, Reading E (2026) Structural dynamics underlying agonist activation of a GLP-1R-Gs precoupled complex. bioRxiv:2026.2008.2003.742488. https://doi.org/10.64898/2026.08.03.742488
76. Tang H, Robinson CV (2024) From G-protein-coupled receptors to solute carriers - mass spectrometry informs dynamics, function, and regulation. Chem 10:2358–2372. https://doi.org/10.1016/j.chempr.2024.02.022
77. Toporowska J, Kapoor P, Musgaard M, Gherbi K, Sengmany K, Qu F, Soave M, Yen H-Y, Hansen K, Jazayeri A, Hopper JTS, Politis A (2024) Ligand-induced conformational changes in the β1-adrenergic receptor revealed by hydrogen-deuterium exchange mass spectrometry. Nat Commun 15:8993. https://doi.org/10.1038/s41467-024-53161-0
78. Vinciauskaite V, Masson Glenn R (2023) Fundamentals of HDX-MS. Essays Biochem 67:301–314. https://doi.org/10.1042/EBC20220111
79. Vo AA, Modak A, Lu S, Blanchard SC, Lambert NA, Robertson MJ (2026) Snapshots of the dynamic basis of NTSR1 G protein subtype promiscuity. Nature 652:803–811. https://doi.org/10.1038/s41586-026-10120-7
80. Wales TE, Engen JR (2006) Hydrogen exchange mass spectrometry for the analysis of protein dynamics. Mass Spectrom Rev 25:158–170. https://doi.org/https://doi.org/10.1002/mas.20064
81. Wang J, Gareri C, Rockman HA (2018) G-Protein–Coupled Receptors in Heart Disease. Circulation Research 123:716–735. https://doi.org/10.1161/CIRCRESAHA.118.311403
82. Warne T, Serrano-Vega MJ, Baker JG, Moukhametzianov R, Edwards PC, Henderson R, Leslie AGW, Tate CG, Schertler GFX (2008) Structure of a β1-adrenergic G-protein-coupled receptor. Nature 454:486–491. https://doi.org/10.1038/nature07101
83. Weigelt J, McBroom-Cerajewski LDB, Schapira M, Zhao Y, Arrowsmith CH (2008) Structural genomics and drug discovery: all in the family. Curr Opin Chem Biol 12:32–39. https://doi.org/https://doi.org/10.1016/j.cbpa.2008.01.045
84. West Graham M, Chien Ellen YT, Katritch V, Gatchalian J, Chalmers Michael J, Stevens Raymond C, Griffin Patrick R (2011) Ligand-Dependent Perturbation of the Conformational Ensemble for the GPCR β<sub > 2 Adrenergic Receptor Revealed by HDX. Structure 19:1424–1432. https://doi.org/10.1016/j.str.2011.08.001
85. Yang L, Yang D, de Graaf C, Moeller A, West GM, Dharmarajan V, Wang C, Siu FY, Song G, Reedtz-Runge S, Pascal BD, Wu B, Potter CS, Zhou H, Griffin PR, Carragher B, Yang H, Wang M-W, Stevens RC, Jiang H (2015) Conformational states of the full-length glucagon receptor. Nat Commun 6:7859. https://doi.org/10.1038/ncomms8859
86. Yen H-Y, Hoi KK, Liko I, Hedger G, Horrell MR, Song W, Wu D, Heine P, Warne T, Lee Y, Carpenter B, Plückthun A, Tate CG, Sansom MSP, Robinson CV (2018) PtdIns(4,5)P2 stabilizes active states of GPCRs and enhances selectivity of G-protein coupling. Nature 559:423–427. https://doi.org/10.1038/s41586-018-0325-6

87. Yen H-Y, Jazayeri A, Robinson CV (2023) G Protein-Coupled Receptor Pharmacology: Insights from Mass Spectrometry. Pharmacol Rev 75:397–415. https://doi.org/10.1124/pharmrev.120.000237
88. Yen H-Y, Liko I, Song W, Kapoor P, Almeida F, Toporowska J, Gherbi K, Hopper JTS, Charlton SJ, Politis A, Sansom MSP, Jazayeri A, Robinson CV (2022) Mass spectrometry captures biased signalling and allosteric modulation of a G-protein-coupled receptor. Nat Chem 14:1375–1382. https://doi.org/10.1038/s41557-022-01041-9
89. Zhang H, Qiao A, Yang D, Yang L, Dai A, de Graaf C, Reedtz-Runge S, Dharmarajan V, Zhang H, Han GW, Grant TD, Sierra RG, Weierstall U, Nelson G, Liu W, Wu Y, Ma L, Cai X, Lin G, Wu X, Geng Z, Dong Y, Song G, Griffin PR, Lau J, Cherezov V, Yang H, Hanson MA, Stevens RC, Zhao Q, Jiang H, Wang M-W, Wu B (2017a) Structure of the full-length glucagon class B G-protein-coupled receptor. Nature 546:259–264. https://doi.org/10.1038/nature22363
90. Zhang M, Chen T, Lu X, Lan X, Chen Z, Lu S (2024) G protein-coupled receptors (GPCRs): advances in structures, mechanisms and drug discovery. Signal Transduction and Targeted Therapy 9:88. https://doi.org/10.1038/s41392-024-01803-6
91. Zhang X, Chien EYT, Chalmers MJ, Pascal BD, Gatchalian J, Stevens RC, Griffin PR (2010) Dynamics of the β2-Adrenergic G-Protein Coupled Receptor Revealed by Hydrogen–Deuterium Exchange. Anal Chem 82:1100–1108. https://doi.org/10.1021/ac902484p
92. Zhang Y, Sun B, Feng D, Hu H, Chu M, Qu Q, Tarrasch JT, Li S, Sun Kobilka T, Kobilka BK, Skiniotis G (2017b) Cryo-EM structure of the activated GLP-1 receptor in complex with a G protein. Nature 546:248–253. https://doi.org/10.1038/nature22394
93. Zivanov J, Nakane T, Forsberg BO, Kimanius D, Hagen WJH, Lindahl E, Scheres SHW (2018) New tools for automated high-resolution cryo-EM structure determination in RELION-3. eLife 7:e42166. https://doi.org/10.7554/eLife.42166

## Figures

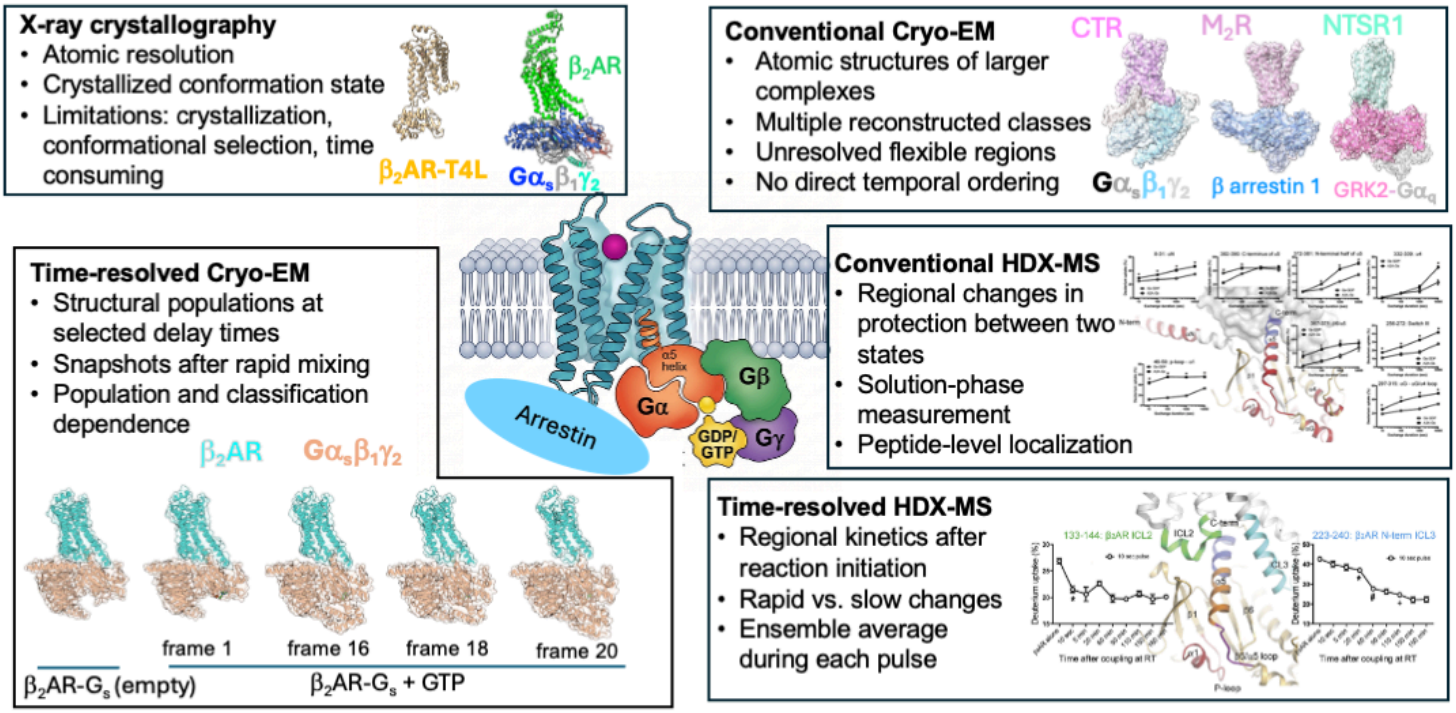


**Figure 1**

**Complementary information provided by high-resolution structural methods and HDX-MS in GPCR research.** X-ray crystallography and conventional cryo-electron microscopy (cryo-EM) define the atomic or near-atomic architecture of selected GPCR conformations, including ligand-binding pockets, activation microswitches, and receptor–transducer interfaces. Time-resolved cryo-EM further resolves structural populations enriched at defined post-trigger time points. Conventional HDX-MS complements these approaches by identifying regional changes in backbone protection between pre-equilibrated functional states, whereas pulse-labeling HDX-MS monitors the reaction-time dependence of these changes using a fixed $D_2O$-labeling pulse. Data of HDX-MS shown in these panels were adapted from Du *et al* (Du et al. 2019) with permission. HDX-MS measurements are ensemble-averaged and peptide-resolved and therefore do not independently define atomic contacts or unique conformational states. The following structures (PDB) were used: X-ray crystal structures of $b_2AR$ (2RH1) (Cherezov et al. 2007), $b_2AR$-$G_s$ complex (3SN6) (Rasmussen et al. 2011b); cryo-EM structures of calcitonin receptor (CTR)-$G_s$ complex (5UZ7) (Liang et al. 2017), $M_2R$- b arrestin 1 complex (6U1N) (Staus et al. 2020), neurotensin receptor 1 (NTSR1) - GRK2 - $G\alpha_q$ complex (8JPB) (Duan et al. 2023); frame 1 of $b_2AR$-$G_s^{EMPTY}$ (8GDZ), frame 1 (8GG3), frame 16 (8GGA), frame 18 (8GGC) and frame 20 (8GGF) of $\beta_2AR$–$G_s^{GTP(Merged)}$ (Papasergi-Scott et al. 2024).

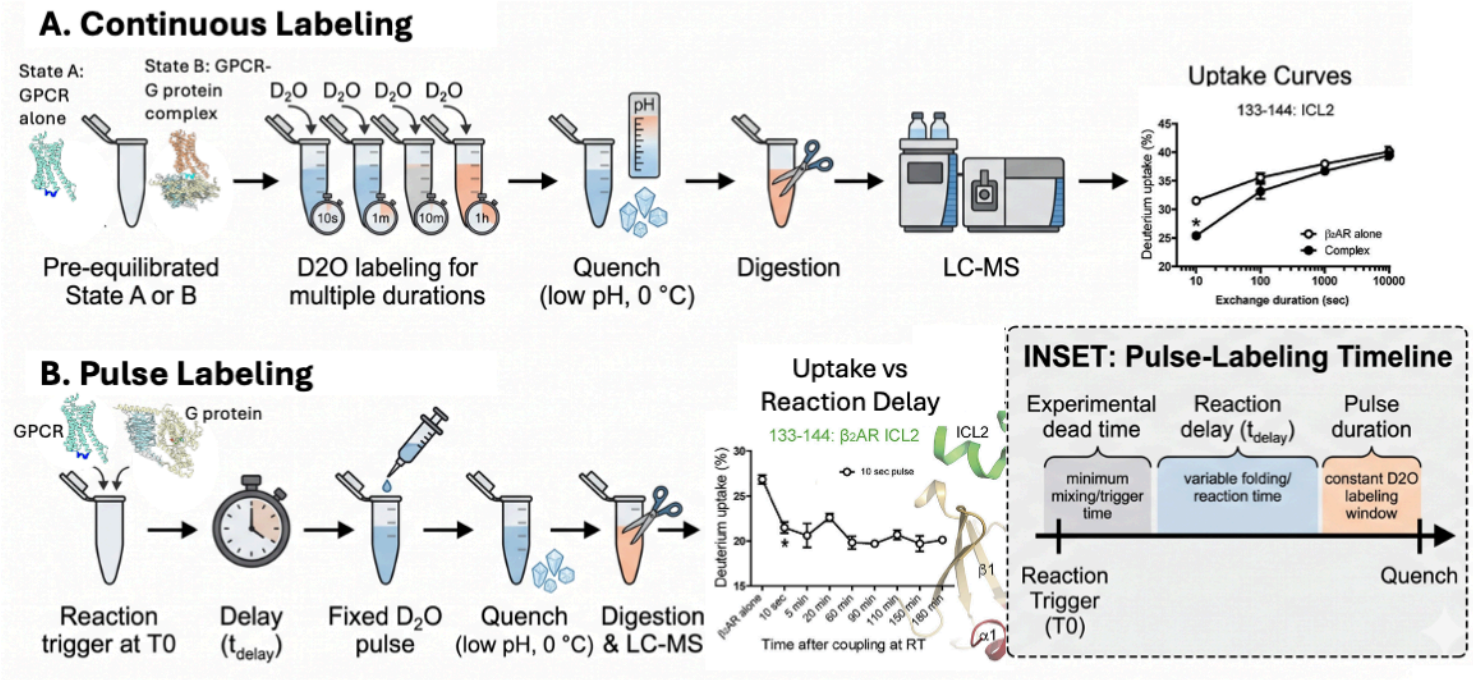


**Figure 2**

**Continuous-labeling and pulse-labeling HDX-MS workflows. (A)** Continuous-labeling HDX-MS compares pre-equilibrated protein states using multiple $D_2O$ exposure times and generates exchange curves as a function of labeling duration. **(B)**Pulse-labeling HDX-MS initiates a biological reaction at $T_0$, introduces a fixed $D_2O$ pulse after defined reaction delays ($t_{delay}$), and monitors the temporal progression of regional protection changes. Both workflows share the downstream quenching, proteolysis, liquid chromatography, mass-spectrometric detection, and data-analysis steps. Pulse-labeling measurements are limited by mixing dead time and provide ensemble-averaged rather than instantaneous structural information. The representative HDX data for continuous labeling and pulse labeling were adapted from Du *et al* (Du et al. 2019) with the permission.

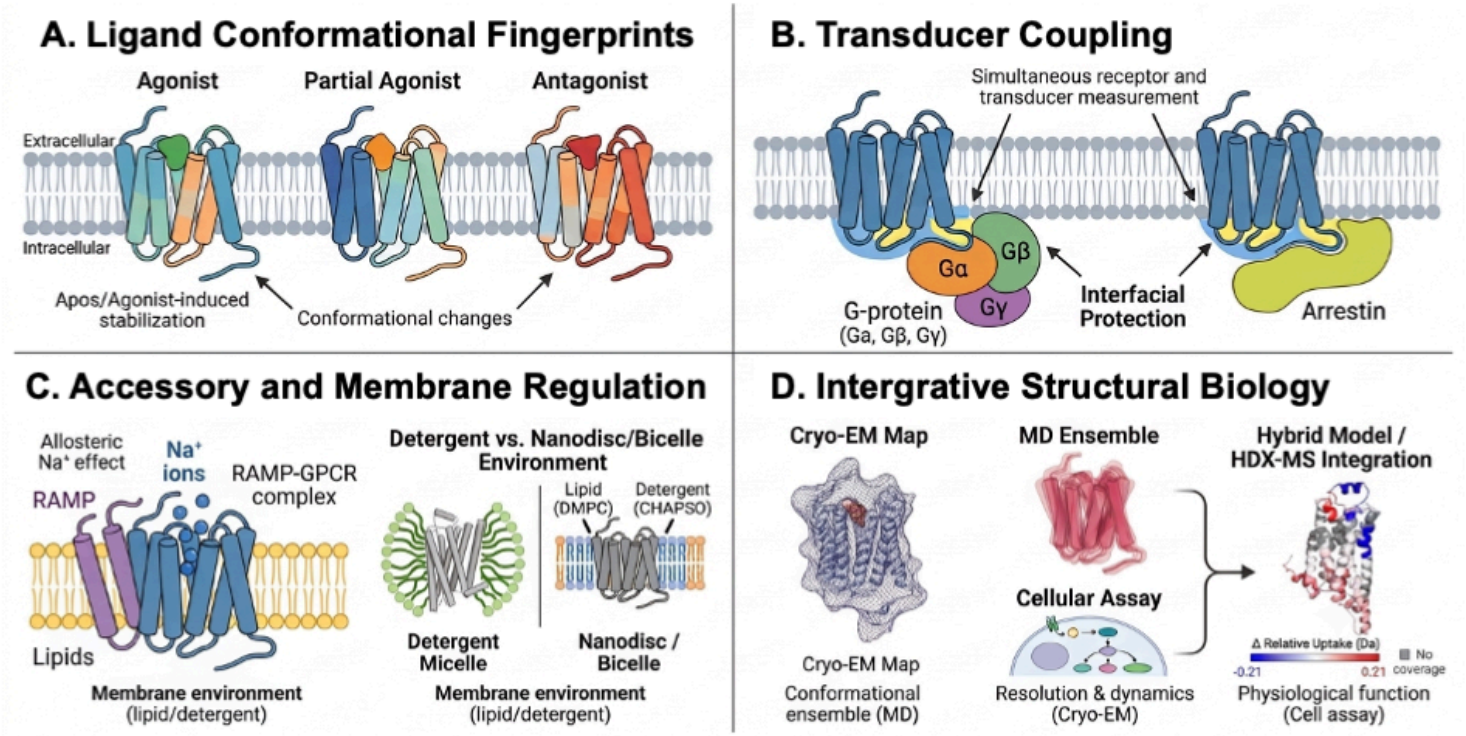


**Figure 3**

**Representative applications of HDX-MS in GPCR structural biology.** HDX-MS can be used to **(A)** map ligand-sensitive regions and define receptor-dependent conformational fingerprints, **(B)** characterize conformational changes associated with G-protein and arrestin coupling, **(C)** examine allosteric regulation by accessory proteins, ions, and membrane environments, and **(D)** constrain structural and computational models through integration with crystallography, cryo-EM, molecular simulations, and functional assays (the HDX-MS profile of $b_1$AR in panel 4 was adapted from Toporowska *et al* (Toporowska et al. 2024) with permission). Changes in deuterium uptake reflect altered regional protection arising from the combined effects of hydrogen bonding, solvent accessibility, and conformational exchange; mechanistic assignments therefore require orthogonal validation.